Advantage and Current Limitations of Advanced Fracture Mechanics for 3D-Integration and BEoL under CPI Aspects

Auersperg, Juergen, Dudek, Rainer, Rzepka, Sven, Michel, Bernd
Fraunhofer ENAS, Micro Materials Center Chemnitz
Technologie-Campus 3, 09126 Chemnitz, Germany
e-mail: juergen.auersperg@enas.fraunhofer.de

Abstract

The ongoing development towards increasing functional density and performance drives the improvement of IC packaging and interconnection technologies. However, new integration technologies, such as through silicon vias (TSVs) for 3D stacking for heterogeneous systems as well as rigid micro-bumps together with the utilization of delicate new (porous ultra low-k) materials weaken the mechanical stability. As a result, the risks of cracking or delaminations increase e.g. in back-end-of-line (BEOL) structures or in the surrounding of TSVs.

Chip package interaction (CPI) under thermal loading, assembly loading as well as residual stresses from different processing steps provide the dominating thermo-mechanical stress situations.

In this field, qualified Finite Element Modeling (FEM) techniques play a well accepted key role to manage damage, cracking and delamination risks in the package design phase and also during failure tolerance optimization. Well defined/measured materials properties, loadings, boundary conditions and residual stresses from manufacturing are preconditions to ensure the quality of simulation results. Unfortunately, stress/strain singularities at certain locations within the designs under investigation call for advanced approaches taking into account the stress singularities, i.e., fracture mechanics approaches, instead.

The contribution explains classic fracture mechanics approaches for bulk fracture and material interface delamination investigations as well as their recently realized extensions and current limitations. In contrast, advanced approaches allowing the simulation of crack initiation and propagation like cohesive zone modeling (CZM) and extended FEM (X-FEM) will be explained and discussed with respect to their advantages/disadvantages. Their benefits for the thermo-mechanical reliability optimization will be explained with the aid of 3D IC-integration, TSV and a smart lighting assembly, in detail.

Bulk Fracture Mechanics

It is common knowledge in mechanical engineering that stresses/strains at locations with field singularities cannot be evaluated by classical strength hypotheses. To come to a conservative evaluation of the structural toughness of present advanced electronic package designs the application of fracture mechanics concepts is the recommended procedure. Otherwise, there are several handicaps – partly overcome by theoretical adjustments – but, rarely implemented in commercial FEM-codes (see Table 1).

Even if most of the J-type integral concepts listed in Table 1 are rather old, these concepts towards nonlinear, rate dependent material behaviors, genuine 3D stress situations, dynamics or large strains are very limited.

Table 1: History of important J-type integral concepts

1968	Rice	J	„small-scale yielding“
1971 1972	Broberg Knowles/ Sternberg		}large strain integrals -“-
1972	Blackburn	J^*	elastic-plastic
1973	Palmer/Rice	J	loaded crack flanks
1975	Eftis/Jones/ Liebowitz	$\tilde{G}$	“large-scale yielding“
1976	Aifantis/ Gerberich	J^*	diffusion problems
1979	Gurtin	L,M	thermo-elastic
1979	Achenbach et al.	l_c	general, dynamic, non-linear
1980	Riedel/Rice et al.	C^*	visco-plastic
1980	Bui/Ehrlacher/ Nguyen	F	heat, dissipation zone
1980	Buggisch/ Gross/Krueger	I_c, Y_m	dynamic, general conservation laws
1981	Atluri	T_c, ΔT_c	creep crack
1981	Sakata/Aoki/ Kishimoto	$\hat{J}$	two-dim. process region
1981	Miyamoto/Kikuchi	$\hat{J}_J$	three-dim. elastic
1982	Xiao/Huang	$J = J_{el} + J_{pl}$	
1983	Will		three-dim. process region
1983	Atluri	T, ΔT, T^*	review article
1983	Ouyang	Y_1	
1984	Will/Michel	J T_J	three-dim. ductile crack, finite process region
1985	Brust/Nishioka/ Nakagaki	T, T^*	very general
1986	Hollstein/Kienzler	R	creep
1988	Shih		three-dim, dyn., monotonic σ-ε curve
1991	Nakagaki	T	strong thermal gradients
1991	Nilsson	$J(s,C)$, J_{tip}	three-dim. J
1992	Rosakis et al.		thermo-mechanical behaviour

Nevertheless, starting with the K-concept which bases on the works of Griffith (1929) [1] and Irwin (1948) [2], J-integral from Rice (1968) [3] and Cherepanov (1967) [4], energy release rate G (‘G’ to honor Griffith) and COD (crack opening displacement) a lot of work was done recently in order to fill up the white areas. The ΔT*-integral – Eq. (1)

$$\Delta T_k^* = \int_\Gamma \left(\Delta W n_k - \left(\sigma_{ij} + \Delta\sigma_{ij} \right) n_j \Delta u_{i,k} \right) d\gamma + \iint_\Omega \left(\frac{1}{2} \Delta\sigma_{ij} \varepsilon_{ij,k} - \Delta\varepsilon_{ij} \left(\sigma_{ij,k} + \frac{1}{2} \Delta\sigma_{ij,k} \right) \right) d\omega$$

with (1)

$$\Delta W = \left(\sigma_{ij} + \frac{1}{2} \Delta\sigma_{ij} \right) \Delta\varepsilon_{ij}$$

from Brust, Atluri et al. [5, 6], is one example which has the potential to take into consideration inelastic behavior of the related materials, but, repaint almost unconsidered for use.

Not to forget, the virtual crack closure technique (VCCT) as derived by Rybicki and Kanninen (1977) [7] from crack closure integral introduced by Irwin (1967) [8] acted as an important step in conjunction with the increasing use of the FEM.

Bi-Material Interface Delamination

Respecting the long and intense history of describing and evaluating the crack tip loading of bi-material interface cracks, we excerpt a summary that illustrates basic conceptions.

Analogous to the bulk fracture stress field description Rice and Shih [9] defined

$$K = K_1 + iK_2 = |K|\, e^{i\psi^*} \tag{2}$$

as the complex stress intensity factor with physical units of $Nm^{-2}\sqrt{m}\ m^{-i\varepsilon}$ and Ψ^* as the phase angle of K. Consequently, the tractions along the interface ahead of the crack tip are given by

$$(\sigma_{xx}^{\infty} + i\sigma_{yy}^{\infty})_{\Theta=0} = Kr^{i\varepsilon} / \sqrt{2\pi r}\ , \tag{3}$$

where the oscillatory exponent ε is

$$\varepsilon = \frac{1}{2\pi}\ln\left[\frac{1-\beta}{1+\beta}\right]$$
$$\kappa_j = \begin{Bmatrix} 3-4\nu_j & plane \quad strain \\ (3-\nu_j)/(1+\nu_j) & plane \quad stress \end{Bmatrix}, \tag{4}$$

with the Dunder's parameters [10]

$$\alpha = \frac{\overline{E}_1 - \overline{E}_2}{\overline{E}_1 + \overline{E}_2} \quad and \quad \beta = \frac{\mu_1(\kappa_2 - 1) - \mu_2(\kappa_1 - 1)}{\mu_1(\kappa_2 + 1) + \mu_2(\kappa_1 + 1)}. \tag{5}$$

Here, μ_j are the shear modules, ν_j Poisson's ratios and subscript j denotes upper and lower material at the interface, respectively. As it is clear from Eq. (2) that K_1 and K_2 do no longer reflect the cracking modes I and II because of the oscillatory term $r^{i\varepsilon}$ and also, the units of this K do not fit into the units of K for bulk material cracking.

That's why: Rice [11] introduced a similar complex stress intensity factor of classical type characterizing the near tip stress field at an interfacial crack with

$$K_I + iK_{II} = K\ l^{i\varepsilon} = |K|\, e^{i\psi}. \tag{6}$$

K_I and K_{II} present the stress intensity factors of the two different crack modes of bi-material fracture, l is an arbitrarily chosen reference length and Ψ is the mode mixity of $K\ l^{i\varepsilon}$. This SIF comes now with physical units of $Nm^{3/2}$ – as known from bulk fracture K. But, K_I, K_{II} as well as Ψ base on the reference length $r=l$. For bi-material cracks with $\varepsilon \neq 0$ they are not directly analogous to mode I and mode II stress intensity factors for bulk materials – a characterizing reference length l needs always to be specified additionally.

The stress field in Eq. (3) can now be rewritten to Eq. (6) and shows clearly the oscillatory nature of the stress fields under LEFM.

$$(\sigma_{xx}^{\infty} + i\sigma_{yy}^{\infty})_{\Theta=0} = \frac{K_I + iK_{II}}{\sqrt{2\pi r}}\left(\frac{r}{l}\right)^{i\varepsilon}. \tag{7}$$

We have now SIFs of different meaning and their related mode mixities Ψ^* and Ψ, for which Rice [11], Hutchinson and Suo [12] and Ikeda et al. [13] found the relations

$$\psi = \psi^* + \varepsilon\ln(l) \quad and \quad \psi_2 = \psi_1 + \varepsilon\ln\left(\frac{l_2}{l_1}\right). \tag{8}$$

Here l_1 and l_2 are two reference lengths for the two mode mixities $\Psi_1 = \Psi_1(l_1)$ and $\Psi_2 = \Psi_1(l_2)$. So, Eq. (8) allows recalculating mode mixities of SIF regarding different reference lengths. As summarized by Agrawal and Karlsson in [13] the most important approaches towards finding the mode mixity regarding VCCT against several approaches towards oscillatory free energy release rates. Furthermore, they discussed the relations between them. Naturally, whereas the underlying theory is even the same, they found the comparability/equality in results or else rather simple relations between them - see also summary and applications by Auersperg et al. [14]. They utilized the formulation of Beuth [15] who introduced a shift-function which approximates the relation between SIF and ERR based phase angles.

As outlined by Sun and Qian [16] and others, there are several approaches to accurately calculate the phase angle regarding SIF or ERR. Although, some of them have the drawback that at least 2 coupled quadratic equations have to be solved for K_I and K_{II}, which requires to select the one solution that makes sense. To overcome this difficulty, Chow and Atluri [17] introduced the so-called coupled energy release rates. They took into account that – in contrast to a crack in homogeneous materials – there is probably no principal stress state in the ligament along the material interface. In 2D the coupled energy release rate is given by

$$G_{I-II} = \frac{1}{2\Delta}\int_0^{\Delta}\left[\sigma_{12}(r)\delta_2(\Delta - r) + \sigma_{22}(r)\delta_1(\Delta - r)\right]dr \tag{9}$$

with the virtual crack extension Δ and the crack opening displacement δi in i-direction. At the end of all calculations the phase angles ψ (for in-plane shear) and φ (for out-of-plane shear) result from 2 separate equations

$$\psi = \tan^{-1}\left(\frac{K_{II}}{K_I}\right) = \tan^{-1}\left(\frac{K_I K_{II}}{K_I^2}\right)$$
$$\varphi = \tan^{-1}\left(\frac{K_{III}}{K_I}\right) = \tan^{-1}\left(\frac{K_I K_{III}}{K_I^2}\right), \tag{10}$$

whereas all mixed and quadratic terms are separately calculated and only one question regarding the sign of K_I is to answer: if the crack is opened – it is positive. Unfortunately, this concept is not yet implemented in a commercial FE-code.

But, there is also good news: ABAQUS™ [18] implementted an interaction integral, a kind of the long time known conservation integrals which was originally invented by Shih and Asaro [19].

Based on the J-integral definition it can be expressed as

$$J_{\text{int}}^{\infty} = \lim_{\Gamma \to 0} \int_{\Gamma} n \cdot M^{\alpha} \cdot q \, d\Gamma$$

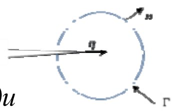

$$M^{\alpha} = \sigma : \varepsilon_{aux}^{\alpha} I - \sigma \cdot \left(\frac{\partial u}{\partial x} \right)_{aux}^{\alpha} - \sigma_{aux}^{\alpha} \cdot \frac{\partial u}{\partial x}, \qquad (11)$$

where Γ is an arbitrary contour surrounding the crack tip, q is a unit vector in the virtual crack extension direction, n is the outward normal on Γ, σ is the stress tensor and u is the displacement vector. The subscription *aux* stands for the auxillary pure fracture modes I, II, and III crack tip fields for $\alpha =$ I,II,III, correspondingly. It is implemented in the finite element code as a domain integral instead of the contour integral shown here and allows the extraction of stress intensity factors by the use of the so-called pre-logarithmic energy factor matrix B [19]

$$J_{\text{int}}^{\alpha} = \int_{A} \lambda(s) n \cdot M^{\alpha} q \, dA \quad and \quad \mathbf{K} = 4\pi \mathbf{B} \cdot J_{\text{int}}, \qquad (12)$$

with dA as a surface element on a vanishingly small tubular surface enclosing the crack tip. Note, that this K is related to Eqs. (2) and (3)!

As results, we have now a *J*-integral value in crack extension direction valid also for bi-material interface cracks together with the stress intensity factors regarding Eq. (2). One question regarding the applicability of the J-integral is: how to consider residual stresses. This can be solved by applying (in bulk fracture case)

$$\bar{J} = \int_{A} \lambda(s) n \cdot \left(W \mathrm{I} - \sigma \cdot \frac{\partial u}{\partial x} \right) \cdot q dA + \int_{V} \sigma : \frac{\partial \varepsilon^{0}}{\partial x} \cdot q dV, \qquad (13)$$

with V as the domain volume enclosing the crack tip or crack front, W is defined as the mechanical strain energy density beside ε^0 which presents the residual strains and remains constant during the entire deformation within the loading step.

Classic Fracture Mechanics - Inputs and Objectives

As previously outlined classic fracture mechanics is always the only instrument to handle singular stress fields.

Input: Prepare the FE-model completely; introduce an initial crack within the FE-model – possibly by means of singular or hybrid elements

Provide: Phase angle sensitive fracture toughness values by experiments

Result: Compare the load dependent fracture parameters (K, J, G for all modes separated) with the fracture toughness's from experiments (K_c, J_c, G_c also for all modes separated) – simplified like

$$\begin{aligned} \Theta_K &= K(\psi) - K_c(\psi) \\ \Theta_G &= G(\varphi) - G_c(\varphi) \\ \Theta_J &= J - J_c \end{aligned} \qquad (14)$$

Thus: Classic fracture mechanics attempts to answer the question whether the loaded sample/design tolerates an initial failure/crack at a critical position or not. Since these results are simply numbers or logics those concepts are able to be utilized within parametric studies or optimization approaches.

In addition, it can also deliver the fracture toughness values necessary for evaluations of crack propagation simulations when applied for fracture experiments with several types of fracture samples.

Nevertheless, a large number of issues is still unsolved or partly solved, at best:

1. Crack flanks under contact pressure, friction
2. Initial stress state (somewhat solved)
3. Alternating stress tractions
4. Cyclic loading conditions and fatigue crack propagation (under investigation)
5. Dynamic loading (shock and vibration)
6. Temperature gradients (somewhat solved)
7. Moisture influence (under investigation)
8. Crack kinking (>90°) and branching
9. Interacting cracks
10. Mode mixity – real loading situation vs. measurement conditions (under investigation)
11. Missing fracture toughness parameter of materials and interfaces → huge amount of measurements necessary.

Sub-BEoL Delamination Surrounding TSVs

While TSV developments continue to attract as the rock star technology of 3D integration, it's important to keep in mind that several delamination and cracking risks mainly driven by the thermal mismatch between copper and silicon have to be solved before transferring 3D integration into production. Especially questions regarding the influence of the expected protrusion of copper on the delamination and cracking risk of BEoL-structures deposited on top of it remain unsolved – see Fig. 1.

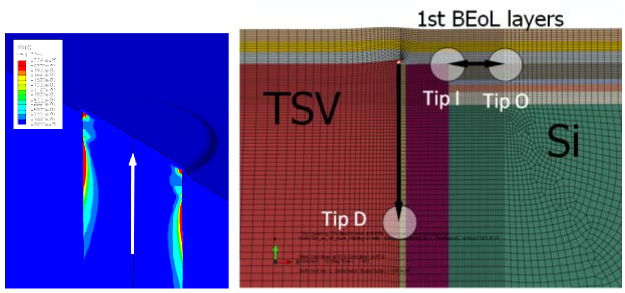

Fig. 1: Plastic strains in a copper-TSV (left) with existing initial delamination underneath 1st BEoL layer (right)

For this subject those classic fracture mechanics concepts seem to deliver good measures for process and design evaluation and optimization – but, handle with care:

- The thermo-mechanical behavior of copper tends to plastic deformations in the range of some 100 % - see also [20].
- Delamination between copper and barrier layers is possible but, the investigation by integral concepts or VCCT is handicapped by the very high plastic deformations in copper.
- So, mode separations fail or come to nothing, as expected.
- Protrusion as a result of high temperatures during BEoL-processing (≈ 430 °C) is highly dependent on the area of those potential delaminations and the initial stress state in copper after its insertion.
- Crack flanks of potential delaminations between several structures of MOL and BEoL close during several steps of

processing – the necessary contact handling conflict with fracture mechanical concepts.

- J-integral or VCCT seem to be unusable for the frequently alternating stresses (direction of traction vector alternates) during several steps of processing - see Fig. 2.

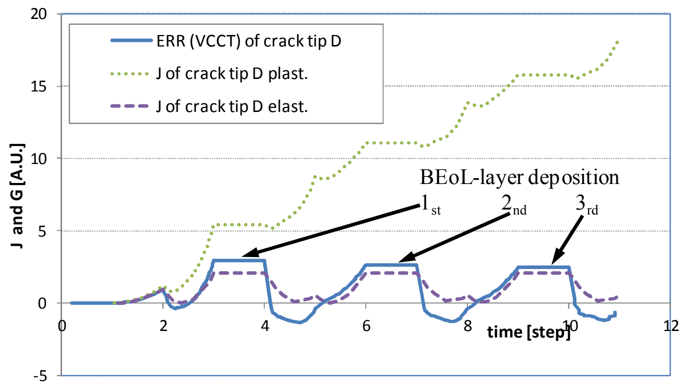

Fig. 2: Jint vs. ERR via VCCT for crack tip D

Crack Initiation and Propagation - CZM

In contrast to classic fracture mechanics concepts newly invented concepts circumvent the explicit preparation of initial cracks. Meant are the cohesive zone method (CZM [21-24]) and the extended FEM (X-FEM [26]) which have the potential of incorporating micromechanical conditions and processes.

As to imagine, there is often no clear crack path or starting position for crack propagation in BEoL-stacks. Otherwise, if the crack probably propagates along a known weak path, cohesive zone/surface modeling (CZM) approaches as introduced by Xu and Needleman [21] or Alfano and Crisfield [22] which are basically enhancements of the approaches of Barenblatt [23] and Dugdale [24] have additionally the potential of incorporating micromechanical conditions and processes whenever with some drawbacks:

- mesh dependence,
- time integration instability, especially at the moment when an allowed peak-stress is achieved and
- large number of model-parameters that have to be measured prior to the simulations – T_{1max}, T_{2max}, T_{3max} (maximum bearable stress levels), G_1, G_2, G_3 (fracture toughness values), β (scheme control parameter), slopes K_a (stiffness until T_{max} is reached).

CZM formulations should incorporate damage evolution and contact/friction handling in order to work in such structures under CPI – see Fig. 3. Notice that the stress singularity known from classic fracture mechanics does not exist at the crack tip for carefully selected parameter sets.

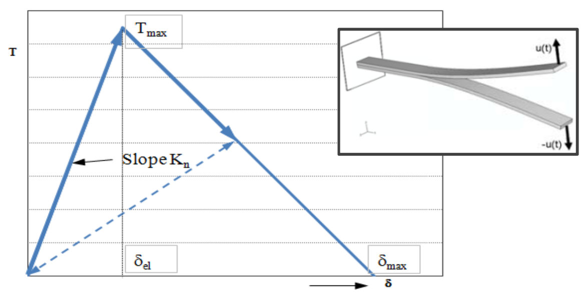

Fig. 3: Traction vs. interface opening in CZM

Cohesive Zone Modeling - Inputs and Objectives

Cohesive zone modeling allows the simulation of crack initiation and propagation.

Input: Prepare the FE-model completely; introduce an initial crack path within the FE-model – by means of cohesive zone elements, no initial crack is necessary. The crack path is not necessarily located within a bi-materials interface!

Provide: Local coordinate system sensitive fracture toughness's, initial stiffness's and maximum traction values from experiments together with time integration stabilization constants

Result: Crack initiation (if the maximum traction value is surpassed) and propagation vs. time along the prepared crack path.

Advantages: There are nearly neither restrictions with regard to constitutive behavior of adjacent materials or the cohesive zone itself nor if geometric nonlinearities (large strains, rotations) play a more or less important role.

X-FEM - Inputs and Objectives

The simulation of crack initiation and propagation through bulk material without taking care of element edges/surfaces or nodes is the purpose of the X-FEM approach. It is introduced by Belytschko et al. [26] as a mesh-less method and uses Heaviside enrichment functions – Eq. (15).

$$u^h(x) = \sum_{I \in N} N_I(x) \left[u_I + H(x) a_I + \sum_{\alpha=1}^{4} F_\alpha(x) b_I^\alpha \right], \qquad (15)$$

were H(x) is the Heaviside enrichment term for nodes belonging to elements cut by the crack and $\sum F_\alpha$ stands for the crack tip asymptotic functions for nodes belonging to elements containing a crack tip – see more in detail in [18]. To perform simulations with X-FEM it is necessary to either use classic, linear elastic fracture mechanics – the VCCT approach – or cohesive damage mechanics for crack initiation and propagation description.

Input: Prepare the FE-model completely; prescribe the initial crack region within the FE-model – no initial crack is to be defined but can be defined.

Provide: Local coordinate system sensitive fracture toughness's, initial stiffness's and maximum traction values from experiments together with time integration stabilization constants

Result: Crack initiation (on locations where the defined maximum traction value is surpassed somewhere) and propagation (direction and rate) vs. time through the X-FEM-region.

Notice: Isotropic, elastic behavior of the material is assumed, at present.

Applicability of the Approaches

Objectives and possible co-working of the concepts discussed above summarized:

- Investigate whether a design under different loading tolerates an initial crack: use classic fracture mechanics (K-concept, J-integral concepts, VCCT-methods)
- Perform parametric studies to find the best solution regarding cracking risk → use classic fracture mechanics approaches. Is the number of unknown parameters sufficiently reduced by relating measurements or knowledge → try CZM

- Determine fracture toughness → use classic fracture mechanics approaches. If the number of unknown parameters is reduced by relating measurements or knowledge → try carefully CZM – see also [25]
- Would like to know where a crack starts, where this crack propagates, which the propagation rate is along a predefined crack path → use CZM
- Would like to know where an interface delamination would start, where it is propagating and which is the propagation rate → use CZM
- Would like to know where a crack would start, where does this crack propagate, which the propagation rate is within a predefined crack region (bulk material) → use X-FEM
- Investigate fatigue crack growth → all concepts are applicable to measure crack initiation, the slope of the PARIS-diagram (Paris, Erdogan [28]) $m = da/dN$ and the number of cycles at crack initiation and total rupture. One exception is that the CZM-concept is not working with a precise located crack tip/front (a stands for the crack length, N is the number of cycles, C and n are constants)

X-FEM - Crack in the Neighborhood of TSVs

In the literature it is widely discussed that copper-TSV causes pumping and protrusion perpendicular to the upper and lower surface as a result of the CTE mismatch between copper and silicon. But, at the same time, the expanding or shrinking copper cause pressure or tension in the surrounding silicon - see explanation in Fig. 4.

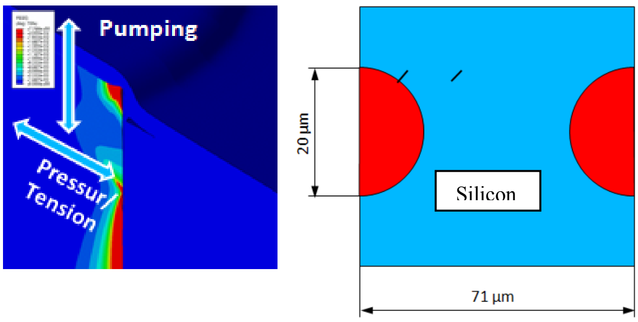

Fig. 4 Role of CTE-mismatch of Cu-TSVs within Si (left), initial crack located between the 2 TSVs (right)

Since this is also the case at room temperature (because of the residual stresses), measurements by means of Raman spectroscopy show increased stress levels close to the TSVs – see also [27].

Additionally, there is probably a cracking risk within the silicon die that has to be evaluated. For this purpose an X-FEM approach was utilized. To perform simulations with X-FEM a cohesive damage mechanics approach for crack initiation and propagation description was used. That's why, a maximum principal stress level together with mixed mode fracture energy properties and damping viscosity were defined for the traction separation law and damage stabilization.

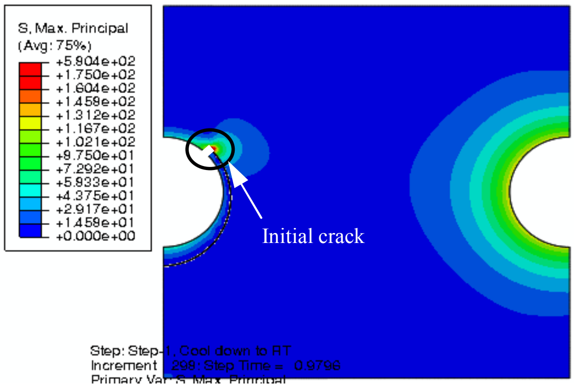

Fig. 5 Initial crack located at the side wall of one TSV; cool down from stress free temperature 160 °C to RT

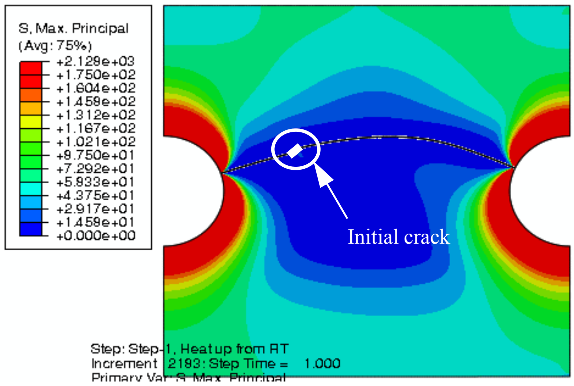

Fig. 6 Initial crack located between the 2 TSVs; heat up from stress free temperature 60 °C to 430 °C

The X-FEM simulations assuming initial cracks at 2 different locations and 2 different initial stress levels show the crack paths as results – see Fig. 5 to Fig. 6.

The model consists of 2 neighboring TSVs and symmetry boundary conditions left plus periodic boundary conditions right and top. The pitch is set to 71 µm and the TSV-diameter is taken as 20 µm. The whole silicon region is prepared for use as X-FEM enrichment region. The copper-TSV and liner/barrier region are suppressed here for better visualization of stress fields and crack paths. Fracture toughness for mode I cracking and the crack initiation stress level had to be reduced in order to force cracking. Looking at the results a bit closer indicates clearly:

1. Cooling down from a higher stress free temperature to RT results in tension within the TSV and tensile stresses perpendicular to the TSV side wall → the crack kinks immediately and surrounds the nearest located TSV independent of its origin – see Fig. 5. Obviously, delamination at the copper-barrier interface is also imaginable.
2. Heating up from a lower stress free temperature results in pressure within the TSV and tensile stresses in silicon perpendicular to the x-axis → the crack opens and propagates into silicon towards the next high tensile stress region (the next TSV) and Fig. 6.

These crack paths look as expected from engineers understanding. Consequently, the crack paths found this way could also help to identify the thermo-mechanics behind an observed failure pattern in the future.

Conclusions

The progress towards increasing functional density and performance drive the improvement of IC packaging and interconnection technologies. 3D stacking for heterogeneous systems, rigid micro-bumps, the utilization of delicate new (porous ultra low-k) materials increase the risks of cracking or delaminations e.g. in back-end-of-line (BEOL) structures or in the surrounding of TSVs. In our paper we have shown that advanced Finite Element Modeling (FEM) techniques can play an important role to manage damage, cracking and delamination risks in the package design phase. The contribution explains classic fracture mechanics approaches for bulk fracture and material interface delamination investigations as well as their newly realized extensions and current limitations. Additionally, advanced approaches allowing the simulation of crack initiation and propagation like cohesive zone modeling and extended FEM were discussed with respect to their advantages/disadvantages. Their benefits for failure tolerance analysis and thermo-mechanical reliability optimization were explained by means of a 3D IC-integration TSV example and a smart lighting assembly, in particular.

Acknowledgments

The authors gratefully acknowledge the Enlight project (http://www.enlight-project.eu/), funded by ENIAC and the German Federal Ministry of Education and Research, for the financial support of some parts of the relating work.

References

1. A. A. Griffith: The Phenomena of Rupture and Flaw in Solids, Philosophical Transactions of the Royal Society London A221, 1929, S. 163-198
2. G. R. Irwin: Fracture Dynamics, Fracturing of Metals, Ed. ASM, Cleveland 1948, S. 147-166
3. J. R. Rice, A Path Independent Integral and the Approximate Analysis of Strain Concentration by Notches and Cracks, Journal of Applied Mechanics, 35, 1968, pp. 379-386.
4. G. P. Cherepanov, The propagation of cracks in a continuous medium, Journal of Applied Mathematics and Mechanics, 31(3), 1967, pp. 503-512.
5. Brust, F. W., Atluri, S. N., 1986, "Studies on Creep Crack Growth using the T*-Integral", Engng. Fract. Mech., 23 (1986)3, pp. 551-574
6. Brust, F. W., Nishioka, T., Atluri, S. N., Nakagaki, M., 1986, "Further Studies on Elastic-Plastic Stable Fracture Utilizing the T*-Integral", Engng. Fract. Mech., 23 (1986)3, pp. 551-574
7. Rybicki EF and Kanninen MF (1977), A finite element calculation of stress intensity factors by a modified crack closure integral, Eng. Fract. Mech. 9, 931–938
8. Irwin. G. R., "Analysis of Stresses and Strains Near the End of a Crack Traversing a Plate,- ASMA Journal of Applied Mechanics, Vol. 24, 1957, pp. 361-364
9. Rice J.R., Sih G.C. (1965) Plane problems of cracks in dissimilar media. J. App Mech 32:418–423
10. Dundurs J. (1969) Edge-bonded dissimilar ortho-gonal elastic wedge. J Appl Mech 36:650–652
11. Rice J. (1988) Elastic fracture mechanics concepts for interface cracks. J. App Mech 55:98–103
12. Hutchinson JW, Suo Z (1992) Mixed mode cracking in layered materials. Adv Appl Mech 29:63–89
13. Ikeda T., Miyazaki N., Soda T. (1998) Mixed mode fracture criterion of interface crack between dissimilar materials. Eng Frac Mech 59(6):725–735
14. Auersperg, J.; Dudek, R.; Oswald, J.; Michel, B., Interaction Integral and Mode Separation for BEoL-cracking and -delamination Investigations under 3D-IC Integration Aspects, , *Proc. 12th Int. Conf. on Thermal, Mechanical & Multi-Physics Simulation and Experiments in Microelectronics and Microsystems,* EuroSimE 2011, Linz, Austria, April 18-20, 2011, on Conf-CD, 068.pdf
15. Beuth J. L. (1996) Separation of crack extension modes in orthotropic delaminationmodels. Int. J of Frac 77: pp. 305–321
16. Sun, C. T., Qian, W., "The Use of Finite Extension Strain Energy Release Rates in Fracture of Interfacial Cracks", Int. J. Solids Structures, Vol. 34. No. 20, pp. 2595-2609
17. Chow, W.T., Atluri, S.N., Finite element calculation of stress intensity factors for interfacial crack using virtual crack closure integral, Comp. Mech. 16 (1995) 417-425
18. SIMULIA (ABAQUS) Manuals (V. 6.11), Dassault Systemes Simula Corp., Providence, RI, USA, 2011
19. Shih, C. F., and R. J. Asaro (1988), "Elastic-Plastic Analysis of Cracks on Bimaterial Interfaces: Part I - Small Scale Yielding," Jour. of Applied Mechanics, pp. 299–316
20. Auersperg, J., Vogel, D., Auerswald, E., Rzepka, S., Michel, B., Nonlinear Copper Behavior of TSV and the Cracking Risks during BEoL-Built-up for 3D-IC-Integration, *Proc. 13th Int. Conf. on Thermal, Mechanical & Multi-Physics Simulation and Experiments in Microelectronics and Microsystems, EuroSimE 2012*, Cascais, Portugal – April 16-17-18, 2012, on CD, IEEE Catalog Number: CFP12566-CDR, ISBN: 978-1-4673-1511-1, papers/123.pdf
21. Xu, X. and Needleman, A., "Numerical Simulations of Fast Crack Growth in Brittle Solids," J. Mech. Phys. Solids, Vol. 42, 1994, pp. 1397–1434
22. Alfano, G. and Crisfield, M.A. Solution strategies for the delamination analysis based on a combination of local-control arc-length and line searches, Int. J. Num. Meth. Engng, 58, 2003, pp. 999-1048
23. Barenblatt, G. I., "The Mathematical Theory of Equilibrium of Cracks in Brittle Fracture," Adv. Appl. Mechanics, 9, 1962, pp. 55–129
24. Dugdale, D. S., "Yielding of Steel Sheets Containing Clits," J. Mech. Phys. Solids, 8, 1960, pp. 100–104
25. J. Auersperg, R. Dudek, B. Brämer, R. Pufall, B. Seiler and B. Michel, Capturing Interface Toughness Parameters from Shear Testing Using Different Fracture Mechanics Approaches, *Proc. 2012 IEEE 14th Electronics Packaging Technology Conference*, 5-7 Dec. 2012, Singapore, on CD, IEEE Catalog Number: CFP12453-USB, ISBN: 978-1-4673-4551-4: /html/315.xml
26. Belytschko T, Moës N, Usui S, Parimi C. Arbitrary discontinuities in finite elements. Int. J. for Numerical Methods in Engineering 2001; 50(4), pp. 993–1013
27. S.-K. Ryu, Q. Zhao, M. Hecker, H.-Y. Son, K.-Y. Byun, J. Im, P. S. Ho, and R. Huang, Micro-Raman spectroscopy and analysis of near-surface stresses in silicon around through-silicon vias for three-dimensional interconnects, *Journ. Appl. Phys*. 111, 063513 (2012); http://dx.doi.org/10.1063/1.369698
28. P Paris and F Erdogan (1963), A critical analysis of crack propa-gation laws, Journal of Basic Engineering, Transactions of the American Society of Mechanical Engineers, December 1963, pp.528-534